Intermediates Relevant to the Carbonylation of Manganese Alkyl Complexes Interrogated by Time Resolved Infrared and Optical Spectroscopy

William T. Boese and Peter C. Ford*

Contribution from the Department of Chemistry, University of California, Santa Barbara, California 93106

Received January 20, 1995[⊗]

Abstract: Intermediates relevant to the carbonylation of metal alkyl complexes have been generated by laser flash photolysis of the manganese acyl complexes $RC(O)Mn(CO)_5$ (R = CH_3, CD_3, CH_2CH_3, CH_2F, CF_3). This results in immediate CO photodissociation to give intermediate acyl complexes which were observed by time resolved infrared (TRIR) and time resolved optical (TRO) spectroscopy. In the presence of added ligands, such intermediates are trapped to form stable *cis*-substituted octahedral complexes in competition with alkyl migration from the acyl group to give the alkyl pentacarbonyl complexes $RMn(CO)_5$. The spectra and reactivity of the intermediate (**I**) derived from $CH_3C(O)Mn(CO)_5$ (**A**) indicate that this exists as the chelated acyl complex (η^2-CH_3CO)$Mn(CO)_4$ in weakly coordinating solvents such as cyclohexane but as the solvento species *cis*-$CH_3C(O)Mn(CO)_4(THF)$ in tetrahydrofuran. Comparisons with thermal reaction kinetics support the assertion that the intermediates generated photochemically are indeed relevant to understanding the mechanism for $CH_3Mn(CO)_5$ carbonylation. The CF_3 and CH_2F analogs of **I** are much more reactive than **I** in cyclohexane solution, and this has been interpreted in terms of the η^2-acyl configuration being destabilized by these electron-withdrawing groups. Solvent effects on the rates of methyl migration and ligand trapping reactions of the intermediate species are described and analyzed in terms of their relevance to the migratory insertion mechanism.

Introduction

The migratory insertion of CO into metal−alkyl bonds is a fundamental reaction of organometallic chemistry and the key carbon−carbon bond-forming step in numerous industrial catalytic carbonylations.[1] While this has been the subject of considerable mechanistic investigation,[2] direct observation of reactive intermediates is limited by low steady state concentrations. Furthermore, the roles of the solvent and of the acyl group in defining the properties of such species, while extensively studied,[2−5] remain to be fully elucidated. Described here is a quantitative investigation utilizing flash photolysis to generate key intermediates and time resolved infrared (TRIR) and time resolved optical (TRO) spectroscopy to probe their structures and reactivities.

The classic model in organometallic chemistry for CO migratory insertion is the carbonylation of $CH_3Mn(CO)_5$ (**M**) (eq 1). Early mechanistic and stereochemical studies[2−4] con-

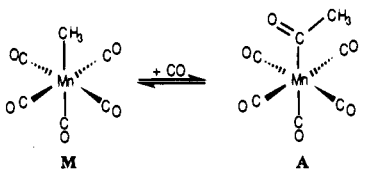

(1)

cluded that this reaction involves migration of the methyl group to the *cis*-CO ligand, followed by trapping of the resulting "unsaturated" acyl intermediate **A′** by carbon monoxide or another ligand L (Scheme 1). Although suggested by kinetics studies,[4] such intermediates have not been detected except in very strongly coordinating solvents.[3d]

In this context, the strategy of the present study was to prepare species having compositions analogous to putative intermediates in various media. For example, photodissociation of CO from the acyl complex **A** (eq 2) would give **I** having the stoichiometry

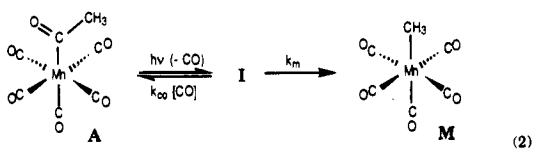

(2)

often proposed for the intermediate initially formed in thermal carbonylation. Rearrangement to **M** would be the microscopic reverse of the first step of carbonylation. TRIR and TRO techniques and low-temperature trapping methods were used to probe the spectra and reactivities of resulting species and the relationship of these to thermal carbonylations.

Experimental Section

Materials. Solvents were purified according to literature procedures and distilled from an appropriate drying agent under nitrogen prior to

[⊗] Abstract published in *Advance ACS Abstracts*, July 15, 1995.

(1) (a) Henrici-Olivé, G.; Olivé, S. *Catalyzed Hydrogenation of Carbon Monoxide*; Springer-Verlag: Berlin, 1984. (b) Parshall, G. W.; Ittle, S. D. *Homogeneous Catalysis*, 2nd ed.; Wiley-Interscience: New York, 1992; Chapter 5.

(2) (a) Collman, J. P.; Hegedus, L. S.; Norton, J. R.; Finke, R. G. *Principles and Applications of Organotransition Metal Chemistry*; University Science Books: Mill Valley , CA, 1987; Chapter 6. (b) Calderazzo, F. *Angew. Chem., Int. Ed. Engl.* **1977**, *16*, 299−311. (c) Wojcicki, A. *Adv. Organomet. Chem.* **1973**, *11*, 87−145. (d) Flood, T. C. *Top. Stereochem.* **1981**, *12*, 37−118.

(3) (a) Calderazzo, F.; Cotton, F. A. *Inorg. Chem.* **1962**, *1*, 30−36. (b) Noack, K.; Calderazzo, F. *J. Organomet. Chem.* **1967**, *10*, 101−104. (c) Flood, T. C.; Jensen, J. E.; Slater, J. A. *J. Am. Chem. Soc.* **1981**, *103*, 4410−4414. (d) Cotton, J. D.; Bent, T. L. *Organometallics* **1991**, *10*, 3156−3160.

(4) Mawby, R. J.; Basolo, F.; Pearson, R. G. *J. Am. Chem. Soc.* **1964**, *86*, 3994−3999.

(5) (a) Wax, M. J.; Bergman, R. G. *J. Am. Chem. Soc.* **1981**, *103*, 7028−7030. (b) Cawse, J. N.; Fiato, R. A.; Pruett, R. L. *J. Organomet. Chem.* **1979**, *172*, 405−413. (c) Webb, S.; Giandomenico, C.; Halpern, J. *J. Am. Chem. Soc.* **1986**, *108*, 345.

0002-7863/95/1517-8381$09.00/0

Scheme 1. Model for Thermal Reaction

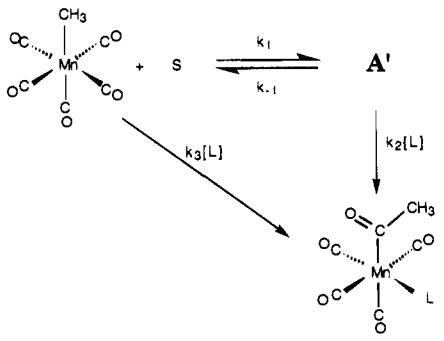

use.[6] Cyclohexane was purchased from Burdick & Jackson, and all other solvents were purchased from Aldrich. Carbon monoxide and CO/Ar gas mixtures were obtained from Liquid Carbonics and passed through an oxygen scrubber and a column of dry 4A molecular sieves. Phosphines, amines, and photosensitizers were used as received from Aldrich. The complexes $CH_3Mn(CO)_5$, $CH_3C(O)Mn(CO)_5$, $CD_3C(O)Mn(CO)_5$, and $CF_3C(O)Mn(CO)_5$ were synthesized by an adaptation of the method of Gladysz;[7] $CH_2FC(O)Mn(CO)_5$ was prepared by the addition of $Na[Mn(CO)_5]$ to freshly prepared and distilled $CH_2FC(O)Cl$.[8] The ^{13}C-labeled product $CH_3{}^{13}C(O)Mn(CO)_5$ was prepared by reaction of $Na[Mn(CO)_5]$ with $CH_3{}^{13}C(O)Cl$.[7]

Spectra. All complexes were characterized by infrared spectroscopy using a Bio-Rad FTS 60 FTIR spectrophotometer. Optical spectra were recorded on a Hewlett-Packard 8452A diode array UV−vis spectrophotometer and emission spectra on a Spex Fluorolog 2 spectrofluorimeter fitted with a water-cooled Hamamatsu R928A photomultiplier tube for detection. Sample solutions were maintained under argon in a 1-cm quartz fluorescence cuvette.

TRIR and TRO Studies. Sample solutions (typical [A] = 1 mM, 50 mL total volume) were prepared by cannula addition of dry distilled solvent to a reservoir fitted with a high-vacuum stopcock and two Ace-Thred electrode adapters with silicone GC septa. Solid manganese complexes were then added to the reservoir against an outward flow of argon. In experiments with added CO, the sample solutions were entrained with pure CO or pre-mixed CO/Ar mixtures. Phosphines and amines were added either by gas-tight syringe through the GC septa or against an outward flow of argon. Care was taken to protect all solutions from extraneous light.

The TRIR apparatus with a XeCl excimer laser (308 nm) as the pulsed excitation source, lead salt diode infrared lasers as probe source, and a Hg/Cd/Te photovoltaic detector has been described.[9] TRIR experiments were carried out on a flowing sample, where the solution was forced through the IR cell from a 50-mL gas-tight syringe with the flow rate controlled by use of a syringe pump. Sufficient flow was maintained to ensure that successive pulses (1 Hz) irradiated fresh solution. Typically data from 25−50 flashes were averaged, a procedure sufficient to ensure good signal-to-noise ratios (>10:1).

TRO experiments were also carried out using the XeCl excimer laser as the excitation source. These employed a quartz flow cell (4 mm × 10 mm path length) with solution replacement achieved with a syringe pump, but when it was necessary to extend observation times to ~0.5 s, flash experiments were carried out on static (non-flowing) samples. A single laser pulse was actuated and the temporal absorbance data were collected. The solution was then replaced and another set of data collected. Several sets of such data were averaged to give a reaction trace used to determine rate constants. The optical probe source was a tungsten/halogen filament lamp whose beam (3-mm diameter) passed through the 10-mm path of the flow cell. The probe beam was overlapped with the excitation beam (2 mm × 8 mm) passing through the 4 mm path length perpendicular to the probe. Wavelength selectivity was obtained with a Digikrom 240 monochromator. The monochromatic probe beam was detected with an IP28 PMT whose signal was amplified and sent to a LeCroy 9400 digital oscilloscope. The detection range was 350−600 nm. The greater sensitivity of the TRO detection system required only 5−10 acquisitions. Data workup was carried out using software custom designed by UGI Scientific.

CW Photolyses. Continuous wave photolysis experiments were carried out using a 200 W focused beam Hg arc lamp. Interference filters were used to isolate single lines of the Hg lamp output. Lamp intensities at 313 and 366 nm were determined using ferrioxalate[10] and Aberchrome 540[11] actinometry, respectively. Sample solutions, deaerated by entraining with the CO/Ar gas mixture of the experiment, were photolyzed in 1-cm quartz fluorescence cuvettes with constant stirring.

Quenching Experiments. Solutions for emission quenching experiments were prepared by gravimetric methods and degassed with Ar in a 1-cm quartz fluorescence cell sealed with a rubber septum. The integrated emission intensities over the 400−550-nm range were measured as a function of [A] to determine Stern−Volmer quenching constants.

Low-Temperature Infrared Experiments. Solutions for low-temperature IR experiments were maintained in an air-tight cell constructed of BeCu with indium O-rings and CaF_2 windows. A path length of 1.0 mm was obtained using a stainless steel spacer. Solutions were syringed into the cell through threaded BeCu ports sealed with silicone rubber septa. The sample cell was fitted to a low-temperature pour-fill dewar/vacuum shroud apparatus purchased from R. G. Hansen Associates. The vacuum shroud was fitted with CaF_2 windows. After the shroud was evacuated and sealed, a CO_2(s)/acetone (−78 °C) mixture was placed and maintained in the dewar. The apparatus was allowed to thermally equilibrate for 15 min. FTIR spectra of the sample were acquired before and after photolysis, typically one shot (50 mJ) from a XeCl excimer laser, using a BIO-RAD FTS-60 spectrometer.

Molecular Mechanics Calculations. Molecular mechanics calculations were carried out on *cis*-$CH_3C(O)Mn(CO)_4$(Sol) species using Cache software on a Macintosh computer. Additions were made to the supplied parameter list of Allinger to account for the manganese interactions.[12] In order to find the global minimum energy conformation, a search was carried out by rotating the solvento ligand and the acetyl group simultaneously and determining the conformations which corresponded to energy minima. The conjugate gradient method was used to minimize energy until convergence within 0.001 kcal/mol was reached.

Thermal Reaction Kinetics. Solutions in dry, freshly distilled THF were prepared in a 1-cm quartz cuvette by addition of $P(OMe)_3$ via gas-tight syringe to a stock solution of $CH_3Mn(CO)_5$ (1.1×10^{-3} M) under Ar. The [$P(OMe)_3$] was varied from 1.2×10^{-2} to 2.3×10^{-1} M. The reaction to form cis-$CH_3Mn(CO)_4(P(OMe)_3)$ was followed at 372 nm, the λ_{max} of the product with T maintained at 25 ± 0.2 °C.

Results

TRIR, FTIR, and TRO Spectra. Continuous photolysis (313 nm) of $CH_3C(O)Mn(CO)_5$ (**A**) at room temperature in various hydrocarbon, halocarbon, and ether solvents resulted in CO loss and formation of **M** with good photochemical efficiency (Φ = 0.60 in cyclohexane under argon).[13] The reaction was strongly inhibited by added CO. Room temper-

(6) Perrin, D. D.; Armarego, W. L. F.; Perrin, D. R. *Purification of Laboratory Chemicals;* Pergamon Press: Oxford, U.K., 1980; p 251.

(7) Gladysz, J. A.; Williams, G. M.; Tam, W.; Johnson, D. L.; Parker, D. W.; Selover, J. C. *Inorg. Chem.* **1979**, *18*, 553−557.

(8) Truce, W. E. *J. Am. Chem. Soc.* **1948**, *70*, 2828.

(9) (a) DiBenedetto, J. A.; Ryba, D. W.; Ford, P. C. *Inorg. Chem.* **1989**, *28*, 3503. (b) Belt, S. T.; Ryba, D. W.; Ford, P. C. *J. Am. Chem. Soc.* **1991**, *113*, 9524−9528. (c) Ford, P. C.; DiBenedetto, J. A.; Ryba, D. W.; Belt, S. T. *SPIE Proc.* **1992**, *1636*, 9−16.

(10) Calvert, J. G.; Pitts, J. N. *Photochemistry*; J. Wiley & Sons: New York, 1967; pp 783−786.

(11) Heller, H.; Langan, J. R. *J. Chem. Soc., Perkins Trans. 2* **1981**, 341−343.

(12) Allinger, N. L. *J. Am. Chem. Soc.* **1977**, *99*, 8127−8134. The MM2 bond stretching parameters (r^0 in Å; force constant in mdyn/Å) used were: Mn−C_{CO} (1.80, 1.9), Mn−C_{acyl} (2.05, 2.2), Mn−O_{thf} (2.25, 1.2), and C_{co}−O_{co} (1.20, 16.5). The MM2 bond bending parameters (angle in deg; force constant in mdyn/Å) used were the following: Mn−C−O_{co} (180.0, 0.25), Mn−C=O_{acyl} (120.0, 0.50), Mn−C_{acyl}−C_{me} (124.4, 0.40), Mn−O_{thf}−C_{thf} (109.5, 0.20).

(13) Boese, W. T.; Lee, B.; Ryba, D. W.; Belt, S. T.; Ford, P. C. *Organometallics* **1993**, *12*, 4739−4741.

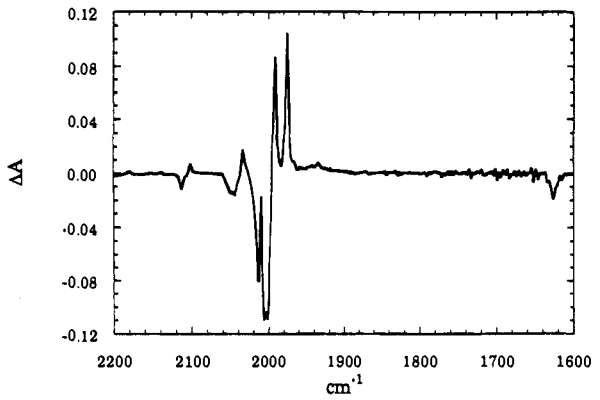

Figure 1. FTIR difference spectrum following 308-nm excimer photolysis of $CH_3{}^{13}C(O)Mn(CO)_5$ in cyclohexane at room temperature. Positive peaks correspond to *cis*-$CH_3Mn(CO)_4(^{13}CO)$.

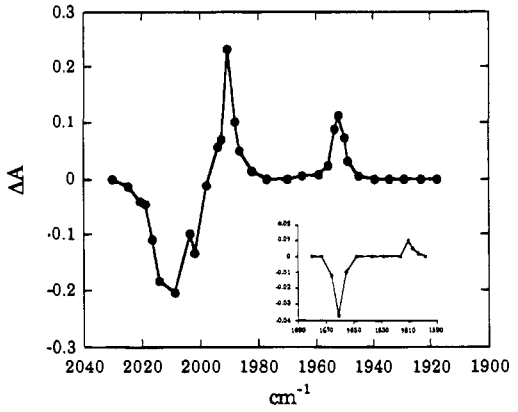

Figure 2. TRIR spectrum 100 μs after 308-nm excitation of 1.0 mM $CH_3C(O)Mn(CO)_5$ in cyclohexane under 1 atm of argon. Inset: Transient IR spectrum in the acyl stretching region acquired using a more concentrated (3.0 mM) solution.

ature photolysis of the labeled complex $CH_3{}^{13}C(O)Mn(CO)_5$ in cyclohexane gave only *cis*- $CH_3Mn(CO)_4(^{13}CO)$ (IR: 2102 (vw), 2033 (m), 2011 (s), 1992 (s), and 1975 (s) cm^{-1})[14] as determined by FTIR spectroscopy (Figure 1), consistent with photolabilization of the *cis*-CO ligand and methyl migration to the vacant site.

When the photolysis was carried out in cyclohexane with 308-nm excitation by a XeCl excimer laser (15 ns pulse, 20–50 mJ/pulse) and monitored by TRIR spectroscopy, IR bands corresponding to **A** (2113 (w), 2051 (m), 2012 (s), 1661 (w) cm^{-1}) were bleached within the shortest possible observation time (~150 ns). A new species (**I**) with IR absorbances at 1991 (s), 1952 (s), and 1607 (w) cm^{-1} was formed promptly (Figure 2). The latter frequencies are not associated with **M**, and they agree well with those found earlier for the photolysis of **A** in a 12 K methane matrix.[15] At ambient temperature **I** did not decay appreciably (<10%) in any solvent during the time window for TRIR detection (up to 1 ms), even under CO (1 atm).

When the TRIR experiment was repeated with $CH_3{}^{13}C(O)Mn(CO)_5$, a modest amount (~10%) of $CH_3Mn(CO)_4(^{13}CO)$ was also found to be formed promptly. (The ^{13}C label separates the product bands and makes them more easily observable.)[16] The concentration of this species did not change measurably up to 1 ms.

Its stability relative to other coordinatively unsaturated complexes[17] allowed **I** to be detected by FTIR spectroscopy following photolysis of **A** in low-temperature solutions. For example, photolysis of **A** (λ_{max} = 285 nm) in 195 K methylcyclohexane gave ν_{CO} bands at 2080 (w), 1988 (s), 1941 (s), and 1607 (w) cm^{-1}, the latter three at frequencies close to those observed for **I** in room temperature cyclohexane. Correspondingly there was an absorbance increase in the visible region of the electronic spectrum with λ_{max} ~ 386 nm. Under these conditions, prompt formation of **M** (as detected by FTIR) was significant (~30%) as seen previously in matrix isolation studies.[15] TRIR and low-temperature FTIR spectra of intermediate **I** in various solvents show good agreement (Table 1).

TRIR spectra of the species initially formed after excimer flash photolysis of **A** in the ether solvents THF, 2-MeTHF, 2,5-Me_2THF, and 2,2,5,5-Me_4THF (Me_4THF) at ambient temperature proved somewhat more complex.[18] At the shortest observation times, three IR bands in the terminal ν_{CO} region were observed. Bands for the predominant species formed (1981 and 1931 cm^{-1} in THF) are analogous to those seen for **I** in cyclohexane, but shifted to lower frequency (Table 1). The third band appears as a shoulder (~1965 cm^{-1} in THF). By analogy to known complexes,[19,20] these data are consistent with formation of *cis* and *trans* isomers of **I** ($\mathbf{I_c}$ and $\mathbf{I_t}$) in an estimated 4 to 1 ratio (see TRO experiments below). Analogous 4/1 formation of *cis/trans*-$CH_3Mn(CO)_4(THF)$ was observed as the photoproduct of 308-nm irradiation of $CH_3Mn(CO)_5$.[19]

Similar spectral changes were observed for 2-MeTHF, 2,5-Me_2THF, and Me_4THF solutions; the respective bands attributed to *trans* isomers appear at ~1965 cm^{-1} in each case except Me_4THF (1962 cm^{-1}). In the Me_xTHF solutions, the band attributed to $\mathbf{I_t}$ underwent first-order decay within a few microseconds with a corresponding intensity increase in the bands attributed to $\mathbf{I_c}$. The k_{obs} values were $(3.3 \pm 0.6) \times 10^4$, $(1.1 \pm 0.2) \times 10^5$, and $(2.4 \pm 0.4) \times 10^5$ s^{-1} in 2-MeTHF, 2,5-Me_2THF, and Me_4THF, respectively. In THF this process was too slow to observe within the available millisecond time window giving $k_{obs} < 1 \times 10^3$ s^{-1}. With this exception, the apparent isomerization from $\mathbf{I_t}$ to $\mathbf{I_c}$ is much faster than subsequent reactions of $\mathbf{I_c}$, so these processes could be treated separately.

Further evidence of the photoproduction of *cis* and *trans* isomers of **I** and subsequent conversion of $\mathbf{I_t}$ to $\mathbf{I_c}$ comes from TRO experiments in 2-MeTHF. Flash photolysis of **A** under CO (0.1 atm) led to transient absorbance over the range 380–450 nm. When monitored at 430 nm, the absorbance decayed via first order kinetics with a rate constant of $(3.5 \pm 0.7) \times 10^4$ s^{-1}, but there was little change at 390 nm. In accord with previous assignments,[19] the ~430-nm absorbance can be attributed to $\mathbf{I_t}$, and its decay rate is in excellent agreement with that of the 1965-cm^{-1} band observed by TRIR.

Kinetics Experiments. Owing to the relatively sluggish reactivity of **I**, it was difficult to use the TRIR method to study the kinetics of methyl migration and of CO trapping at room

(14) Noack, K. *J. Organomet. Chem.* **1968**, *12*, 181–186.
(15) (a) McHugh, T. M; Rest, A. J. *J. Chem. Soc., Dalton Trans.* **1980**, 2323–2332. (b) Hitam, R. B.; Narayanaswamy, R.; Rest, A. J. *J. Chem Soc., Dalton Trans.* **1983**, 615–618.
(16) Coincidental overlap of the IR bands of **A**, **I**, and **M** resulted in difficulty in assessing the extent of "prompt" formation of **M** in the room temperature TRIR experiments. Use of $CH_3{}^{13}C(O)Mn(CO)_5$ resulted in formation of *cis*-$CH_3Mn(CO)_4(^{13}CO)$ with an IR band at 1975 cm^{-1} making it easily distinguishable from **I**.
(17) Ford, P. C.; Boese, W.; Lee, B.; MacFarlane, K. Photocatalysis Involving Metal Carbonyls. In *Photosensitization and Photocatalysis by Inorganic and Organometallic Compounds*; Graetzel, M., Kalyanasundaram, K., Eds.; Kluwer Academic Publishers: The Netherlands, 1993' pp 359–390 and references therein.
(18) In the ether solvents, IR bands are broader and less resolved than in cyclohexane, a feature which may have obscured prompt formation of **M**.
(19) Boese, W. T.; Ford, P. C. *Organometallics* **1994**, *13*, 3525–3531
(20) (a) Noack, K.; Ruch, M.; Calderazzo, F. *Inorg. Chem.* **1968**, *7*, 345–349. (b) Kraihanzel, C. S.; Maples, P. K. *Inorg. Chem.* **1968**, *9*, 1806–1815.

Table 1. Carbonyl Bands (ν_{co} Values in cm^{-1}) for Intermediate **I** formed by 308-nm excitation of A^A in Various Solvents at Ambient T and at −78 °C As Measured by TRIR and FTIR, Respectively

solvent[b]	ν_{co} (296 K)[c]	ν_{co} (195 K)[d]
perfluoromethylcyclohexane	1997, 1959	2083 (w), 1998, 1958
cyclohexane[d]	1990, 1952, 1607(w)	
methylcyclohexane	1990, 1952	2080(w), 1988, 1941, 1607(w)
dichloromethane	1987 (br), 1940 (br)	
toluene	1984 (br), 1941 (br)	
tetrahydrofuran	1981 (br), 1931 (br)	2077(w), 1977, 1928, 1602(w)
2-MeTHF	1979 (br), 1932 (br)	2077(w), 1977, 1928, 1600(w)
2,5-Me_2THF	1982 (br), 1932 (br)	2077(w), 1979, 1931, 1603(w)
2,2,5,5-Me_4THF	1984 (br), 1945 (br)	

[a] The CO stretching frequencies for **A** are 2110, 2051, 2012, and 1661 and they are independent of solvent. Some of these IR data were reported in a preliminary communication.[13] [b] All solvents were dried and redistilled before use. [c] Room temperature data were taken from TRIR spectra 100 μs after 308 nm flash excitation. [d] Low-temperature data were recorded on a Bio-Rad FTS-60 FTIR spectrometer immediately after 308 nm excitation with one pulse from an XeCl excimer laser.

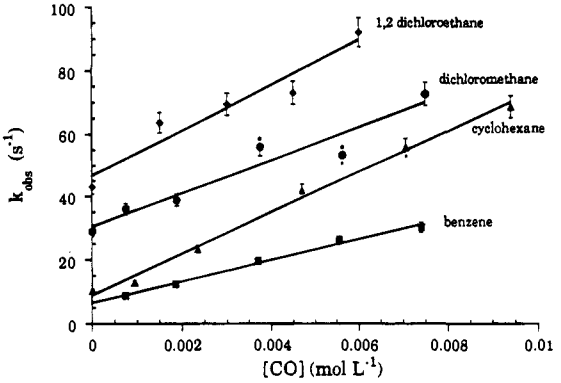

Figure 3. Plots of the observed rate constants for decay of **I** monitored at 400 nm in various solvents as a function of [CO].

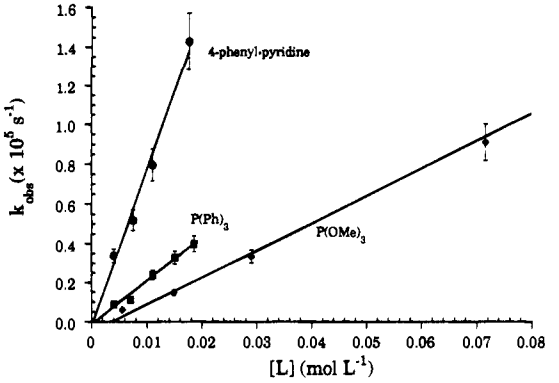

Figure 4. T3RIR spectral changes following 308-nm photolysis of **A** in cyclohexane in the presence of 6.0 mM 4-phenylpyridine. Spectra are spaced at 4-μs intervals.

Table 2. Rate constants for CO Addition (k_{co}) and Methyl Migration (k_m) Reactions of **I** in Various Solvents Determined from Optical Flash Photolysis Experiments[a]

solvent	ϵ^b	k_{co}[c] (M^{-1} s^{-1})	k_m (s^{-1})
perfluoromethylcylohexane		$(1.5 \pm 0.2) \times 10^4$	< 1.0
benzene	2.3	$(3.3 \pm 0.3) \times 10^3$	6.7 ± 0.7
cyclohexane	2.0	$(6.5 \pm 0.7) \times 10^3$	9.0 ± 0.9
dichloromethane	9.1	$(5.3 \pm 0.5) \times 10^3$	30.4 ± 3.0
1,2-dichloroethane	10.7	$(7.3 \pm 0.7) \times 10^3$	46.8 ± 4.7

[a] Conditions: [**A**] = 5 × 10^{-4} M, [CO] = 0−1 × 10^{-2} M, room temperature. [b] *Handbook of Chemistry and Physics,* 63rd ed.; CRC Press: Boca Raton, FL, 1982; pp E-51−53. [c] Concentrations of CO in various solvents were corrected for differences in solubility: *IUPAC Solubility Data Series: Carbon Monoxide;* Cargill, R. W., Ed.; Pergamon Press: New York, 1990; Vol. 43.

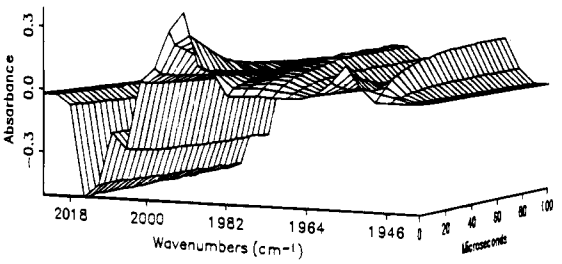

Figure 5. Temporal IR absorbance changes corresponding to the loss of **I** (1991 cm^{-1}) and formation of *cis*-$CH_3C(O)Mn(CO)_4$(4-Ph-py) (1979 cm^{-1}).

temperature (the necessity for a flowing sample solution imposed an upper time limit of ~1 ms). Therefore, TRO experiments with a longer time window (0.5 s) were carried out. These demonstrated the prompt formation of **I** followed by exponential decay over several milliseconds. The k_{obs} values determined proved to be dependent on both [CO] and the media.

According to the model described by eq 2, the rate of disappearance of **I** at a fixed [CO] is the sum of the CO substitution and methyl migration terms:

$$-d[\mathbf{I}]/dt = k_{obs}[\mathbf{I}] = (k_{co}[CO] + k_m)[\mathbf{I}] \quad (3)$$

Thus, a plot of k_{obs} versus [CO] should be linear with a nonzero intercept equal to the first-order rate constant for methyl migration (k_m). The slope would be k_{co}, the second-order rate constant for CO substitution. Such relationships were indeed observed in weakly coordinating solvents (Figure 3) and the k_m and k_{co} values obtained in several hydrocarbon and halocarbon solvents are summarized in Table 2. The k_{co} values determined for these systems proved to be relatively insensitive to solvent, ranging from 3.3 × 10^3 M^{-1} s^{-1} in benzene to 1.5 × 10^4 M^{-1} s^{-1} in PFMC. In contrast, the methyl migration pathway was much more solvent sensitive; k_m varied by more than a factor of 50, and the weakest coordinating solvent (PFMC) displayed the smallest value.

The reactivity of **I** with more nucleophilic ligands (L), such as PPh_3, $P(OMe)_3$, and 4-phenylpyridine (Ph-py) in cyclohexane, was much higher, and these reactions led to substituted acyl complexes $\mathbf{A_L}$ with IR spectra consistent with a *cis* stereochemistry in each case.[20b]

$$\mathbf{I} + L \xrightarrow{k_L} cis\text{-}CH_3C(O)Mn(CO)_4(L) \quad (4)$$

TRIR spectra were constructed by carrying out the flash experiment at a series of incrementally varied detection frequencies and assembling a composite of the ν_{co} region (Figure 4). Product formation occurred concomitantly with loss of **I** via pseudo-first-order kinetics in excess L (Figure 5), and good agreement was observed between TRIR product spectra and FTIR spectra obtained from solutions at the end of the photolysis

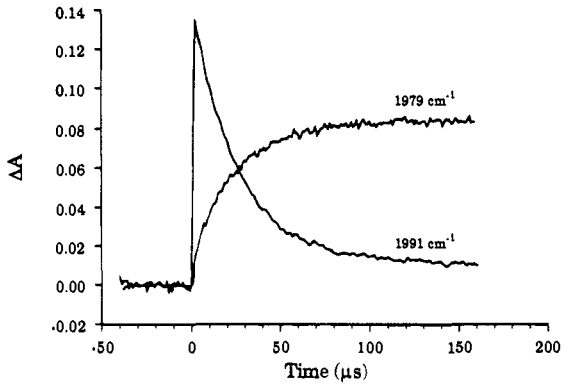

Figure 6. Plots of the observed rate constants for the decay of **I** in cyclohexane as a function of ligand concentration [L] as determined by TRIR.

Table 3. The Reactivity of **I** with Various L in Cyclohexane, PFMC and THF. Comparison of the Reactivity of **I** vs That of the $CH_3Mn(CO)_4(Sol)$ Analog under Similar Conditions[a]

		k_L ($M^{-1}s^{-1}$)	
solvent	ligand	**I**	$CH_3Mn(CO)_4(Sol)$[b]
cyclohexane	Phpy	$(7.5 \pm 1.5) \times 10^6$	$(2.5 \pm 0.3) \times 10^9$
cyclohexane	$P(Ph)_3$	$(2.3 \pm 0.5) \times 10^6$	$(1.0 \pm 0.2) \times 10^9$
cyclohexane	$P(OMe)_3$	$(1.4 \pm 0.3) \times 10^6$	$(1.1 \pm 0.2) \times 10^9$
cyclohexane	CO	$(6.5 \pm 1.3) \times 10^3$	$(4.5 \pm 0.5) \times 10^8$
PFMC	CO	$(1.5 \pm 0.3) \times 10^4$	$(1.0 \pm 0.5) \times 10^{10}$
THF	CO	$< 5 \times 10^2$	$(1.4 \pm 0.3) \times 10^2$

[a] Conditions: [A] = 1×10^{-3} M, [Ph-py] = 4.0×10^{-3} to 1.8×10^{-2} M, [$P(Ph)_3$] = 4.0×10^{-3} to 1.5×10^{-2} M, [$P(OMe)_3$] = 6.0×10^{-3} to 1.5×10^{-1} M, [CO] = 1.0×10^{-3} to 1.0×10^{-2} M, room temperature. [b] Values are those reported in ref 15.

experiment. In excess L, plots of the k_{obs} versus [L] for disappearance of **I** (Figure 6) and for appearance of *cis*-$\mathbf{A_L}$ were linear with intercepts near the origin since the k_m term would have been but a small component of the overall rates under the experimental conditions. Slopes of these plots gave the k_L's for substitution by the various ligands in cyclohexane (Table 3).

Reaction of **I** with CO in THF was too slow to observe by either TRO or TRIR techniques even under $P_{co} = 1$ atm. Slow formation of **M** was observed and a k_m of 8.8 ± 1 s^{-1} was determined in the absence of added CO. Under $P_{co} = 1.0$ atm ([CO] ~ 0.008 M), k_{obs} was marginally higher, but the increase was not sufficiently outside experimental uncertainty to attribute confidently to a k_{co}[CO] contribution. From these observations, the upper limit for k_{co} in THF was calculated to be $\sim 5 \times 10^2$ M^{-1} s^{-1}. In this context it is worth noting that the quantum yield for the **A** → **M** transformation under continuous photolysis decreased from 0.60 under Ar to 0.45 under CO (1 atm). On the basis of the model shown in eq 2, this suggests a $k_{co} \sim 4 \times 10^2$ M^{-1} s^{-1} in reasonable agreement with the above upper limit.

Relative reactivities of **I** in different THF solvents (in these cases the *cis* isomers $\mathbf{I_c}$) were evaluated by using TRO detection to examine the disappearance of **I** in the presence of added $P(OMe)_3$, since this occurred on a convenient time scale. This reaction gave a mixture of the *cis*-substituted acyl product plus **M**. In analogy to eq 3, a linear relationship between k_{obs} and [L] was obtained.

$$-d[\mathbf{I}]/dt = k_{obs}[\mathbf{I}] = (k_L[L] + k_m)[\mathbf{I}] \quad (5)$$

The intercepts of these plots represent the k_m's for methyl migration, and the slopes represent the k_L values for $P(OMe)_3$ substitution in the respective solvents (Table 4). In 2-MeTHF and 2,5-Me_2THF solutions the k_L values were essentially

Table 4. Rate Constants for $P(OMe)_3$ Addition (k_L) and Methyl Migration (k_m) Reactions of **I** in Ether Solvents[a]

solvent	k_L (M^{-1} s^{-1})	k_m (s^{-1})
THF	$(1.7 \pm 0.3) \times 10^3$	9.3 ± 1.9
2-MeTHF	$(3.6 \pm 0.7) \times 10^3$	4.4 ± 0.9
2,5-Me_2THF	$(1.9 \pm 0.4) \times 10^3$	1.6 ± 0.3
Me_4THF	$\sim 6 \times 10^5$	
cyclohexane	1.4×10^6	9.0 ± 0.9

[a] Conditions: [A] = 5×10^{-4} M, [$P(OMe)_3$] = $0-1 \times 10^{-2}$ M, 25 °C.

unchanged, but k_m values decreased with the increasing steric bulk of the solvent. Added CO (1 atm) did not affect k_{obs} in either solvent, thus the upper limit for k_{co} can be estimated as $< 5 \times 10^2$ M^{-1} s^{-1} in these media as well.

The behavior in Me_4THF solutions was somewhat different. In the absence of added ligand, $\mathbf{I_c}$ underwent a subsequent first-order reaction ($k_{obs} \sim (2 \pm 0.5) \times 10^4$ s^{-1}) to give a species with a similar IR spectrum but with the ν_{co} bands shifted ~7 cm^{-1} to lower frequency. The origin of this reaction was unclear, but it appears likely that it was due to the presence of solvent impurities.[21] Nonetheless, the substitution reactivity of other ligands with **I** could be probed by examining the rates with [L] in sufficient excess that reaction with the impurity was not significantly competitive. When this was done using the TRIR technique, k_L values for reactions with $P(OMe)_3$ ($\sim 6 \times 10^5$ M^{-1} s^{-1}) and Phpy (3×10^6 M^{-1} s^{-1}) proved to be much closer to those seen in cyclohexane than in THF.

Other RC(O)M(CO)$_5$ Complexes. In order to evaluate the role of the migrating group, the reactivities of transients generated via photolysis of the complexes $CD_3C(O)Mn(CO)_5$ ($\mathbf{A_{D3}}$), $C_2H_5C(O)Mn(CO)_5$ ($\mathbf{A_P}$), $CF_3C(O)Mn(CO)_5$ ($\mathbf{A_{F3}}$), and $CH_2FC(O)Mn(CO)_5$ ($\mathbf{A_F}$) were evaluated. For $\mathbf{I_{D3}}$, the TRO kinetics experiment in cyclohexane under CO gave k_{co} and k_m values within experimental uncertainties of those determined for **I**. The TRIR spectra of $\mathbf{I_{D3}}$ and **I** were also identical within error. Very similar rates were obtained for the intermediate derived from the closely related propionyl complex $\mathbf{A_P}$ in cyclohexane. Analysis as above gave $k_{co} = 3.3 \times 10^3$ $M^{-1}s^{-1}$ and $k_m = 5.8$ s^{-1}.

Continuous photolysis (313 nm) of $\mathbf{A_{F3}}$ in 296 K cyclohexane with FTIR monitoring resulted in bleaching of the parent IR bands (2118 (w), 2038 (s), 2017 (m), 1656 (w) cm^{-1}) and clean formation of $CF_3Mn(CO)_5$ ($\mathbf{M_{F3}}$, 2119 (w), 2047 (s), 2022 (m) cm^{-1}). XeCl excimer laser photolysis of $\mathbf{A_{F3}}$ in this medium led to a transient species $\mathbf{I_{F3}}$ which displayed TRIR bands at 2054 (s), 2013 (m), 2007 (m), 1976 (s), and 1617 (w) cm^{-1} (Figure 7) and proved to be much more reactive than **I** under analogous conditions. Under argon, $\mathbf{I_{F3}}$ decayed exponentially to give $\mathbf{M_{F3}}$ with $k_{obs} = 2.5 \times 10^4$ s^{-1}. Under CO it disappeared following P_{co} dependent first-order kinetics concomitant with the formation of $\mathbf{M_{F3}}$ and reformation of $\mathbf{A_{F3}}$ in accord with the scheme depicted by eq 6. A plot of k_{obs} (for disappearance

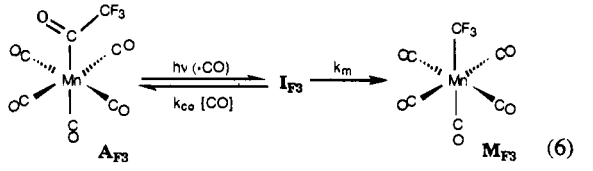

(6)

of $\mathbf{I_{F3}}$) as a function of [CO] (Figure 8) proved linear with a

(21) According to specifications, the commercially available Me_4THF is 97% pure. Although distilled several times, the material used in these experiments contained at least one impurity, which was shown by GCMS to have the same apparent molecular weight as the bulk solvent. It is suspected that this is a less sterically hindered isomer of Me_4THF.

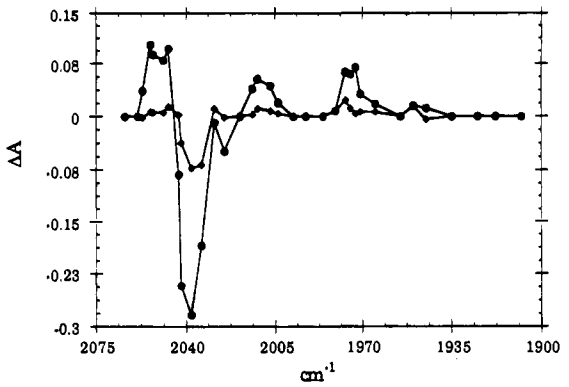

Figure 7. TRIR spectral changes immediately following 308-nm photolysis of $CF_3C(O)Mn(CO)_5$ in cyclohexane under 1 atm of CO.

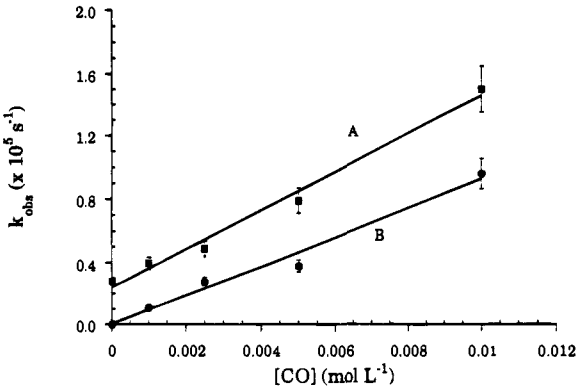

Figure 8. Plots for the reactions of $CF_3C(O)Mn(CO)_4(c\text{-}C_6H_{12})$ with 1 atm of CO in cyclohexane: (A) k_{obs} for the disappearance of $CF_3C(O)Mn(CO)_4(C_6H_{12})$; (B) k_{obs} for the reformation of $CF_3C(O)Mn(CO)_5$. The difference in intercepts corresponds to the CF_3 migration pathway in the absence of CO.

slope corresponding to the k_{co} for CO addition (1.1×10^7 M^{-1} s^{-1}) and a non-zero intercept representing the k_m for CF_3 migration (2.6×10^4 s^{-1}), both much larger than the respective terms noted for **I** in analogous cyclohexane solutions.

In contrast to its relatively high reactivity in cyclohexane, $\mathbf{I_{F3}}$ does not decay appreciably on the TRIR time scale when generated in THF even under CO (1 atm). The TRIR ν_{co} bands were also shifted to considerably lower frequencies (broad bands centered at 2005 and 1965 cm^{-1}). Analogous kinetic behavior and a very similar TRIR spectrum were obtained when the experiment was repeated in Me_2THF (2004 and 1968 cm^{-1}).

Flash photolysis (308 nm) of the related monofluoroacetyl complex $\mathbf{A_F}$ in cyclohexane solution also led to a transient ($\mathbf{I_F}$) which reacted very rapidly with CO. A plot of k_{obs} vs [CO] gave rate constants of 1.2×10^6 M^{-1} s^{-1} for CO addition and 3.3×10^3 s^{-1} for alkyl migration. The ν_{co} bands in the TRIR spectrum of $\mathbf{I_F}$ in cyclohexane, 2052 (s), 2002 (m), 1987 (m), 1966 (s) cm^{-1}, occur at somewhat lower frequency than those of $\mathbf{I_{F3}}$, presumably because of the increased donor ability of CH_2F vs CF_3. Nonetheless, the similar reactivities of these fluorine-substituted transients suggests that $\mathbf{I_F}$ and $\mathbf{I_{F3}}$ have analogous structures in solution.

Photosensitization Experiments. In order to examine the properties of transient **I** when generated other than by direct photolysis of the acetyl complex **A**, the process described in eq 2 was effected with a photosensitizer.[22] Irradiation of a 1.0 mM solution of **A** at 366 nm (ϵ = 250 M^{-1} cm^{-1}) in cyclohexane under Ar resulted in formation of **M** with Φ = 0.14 ± 0.05 as determined by IR spectroscopy. When the experiment was repeated in the presence of 0.8 mM anthracene (ϵ = 1900 M^{-1} cm^{-1} at 366 nm), the quantum yield for sensitized formation of **M** was essentially the same, 0.11 ± 0.04. When photosensitization was carried out in 10:1 cyclohexane–toluene with 1 mM **A** and 15 mM anthracene, prompt (<150 ns) bleaching of **A** and formation of **I** were observed by TRIR in exact analogy to the direct photolysis experiments. The yield of **I** was about 20× higher than would have been the case for the direct absorption of light by **A** under these conditions. Similar 308-nm photolysis of **A** (1.0 mM) in the presence of anthracene (0.6 mM) in a 97:3 methylcyclohexane–toluene solution at −78 °C also resulted in prompt formation of **I** and **M** in a ratio (2.2:1.0) close to that formed in the absence of photosensitizer. These experiments suggest that the direct photolysis and photosensitized reactions proceed via formation of the same excited state(s) of **A** and that prompt formation of intermediate **I** and of **M** are competitive pathways for this state.

The effectiveness of energy transfer from photoexcited anthracene was demonstrated by determining the quenching of fluorescence from a 1.2 mM solution of anthracene in cyclohexane (λ_{max} = 448, 478 nm; λ_{ex} = 355 nm). Incremental additions of **A** to the solution ([**A**] = 0.0–7.0 mM) resulted in a gradual decrease in the integrated emission intensity over the range 400–550 nm. A Stern–Volmer plot of intensity vs [**A**] gave a quenching constant of 1.1×10^{10} M^{-1} s^{-1} based on the reported 12.9-ns fluorescence lifetime of anthracene in cyclohexane.[23,24]

Thermal Reaction of $CH_3Mn(CO)_5$ with $P(OMe)_3$ in THF. The thermal reaction of **M** with $P(OMe)_3$ was investigated in order to provide comparative thermal and photochemical data under closely analogous conditions. The kinetics of reactions of **M** with other L to give the respective acetyl complexes *cis*-$CH_3C(O)Mn(CO)_4L$ in various solvents were studied by Mawby, Basolo, and Pearson.[4] They interpreted their data in terms of the model illustrated in Scheme 1, which would give the following relationship between k_{obs} and [L].

$$k_{obs} = \frac{k_1 k_2[L]}{k_{-1} + k_2[L]} + k_3[L] \qquad (7)$$

In THF k_{obs} was found to reach a limiting value at high [L] independent of the nature of L, and double reciprocal plots of k_{obs}^{-1} vs $[L]^{-1}$ in THF were linear with non-zero intercepts.[4] Thus, the $k_3[L]$ term for direct reaction of L with **M** must be very small in this solvent. Values of k_1 and the ratio k_{-1}/k_2 were obtained for various L from the slopes and intercepts of such plots.[4]

In order to compare to the photochemical experiment, the thermal reaction of **M** (1.1×10^{-3} M) with $P(OMe)_3$ (1.2×10^{-2} to 2.3×10^{-1} M) in 25 °C THF was investigated. At all [$P(OMe)_3$] studied, pseudo-first-order kinetics were observed for the formation of *cis*-$CH_3C(O)Mn(CO)_4(P(OMe)_3)$. Treating the ensemble of k_{obs} values in the same manner as above gave a linear plot of k_{obs}^{-1} vs $[L]^{-1}$ from which was determined k_1 = (8.5 ± 0.9) $\times 10^{-4}$ s^{-1} and k_{-1}/k_2 = (6.6 ± 1.3) $\times 10^{-3}$ M. The former is in good agreement with the average k_1 value (9.6×10^{-4} s^{-1}) previously obtained for reactions with other L.[4]

The thermal reaction of **M** with $P(OMe)_3$ (4.5×10^{-2} to 1.5×10^{-1} M) was also investigated in cyclohexane solution and found to be much slower than in THF. In contrast to the THF

(22) Photoejection of CO from related metal carbonyl complexes has been recently demonstrated with the use of photosensitizers, e.g.: Nayak, S. K.; Farrell, G. J.; Burkey, T. J. *Inorg. Chem.* **1994**, *33*, 2236–2242.

(23) Berlman, I. B. *Handbook of Fluorescence Spectra of Aromatic Molecules*; Academic Press: New York, 1965; p 123.

(24) The singlet energy of anthracene is 76.3 kcal mol^{-1} (*Handbook of Organic Photochemistry;* Scaiano, J. C., Ed.; CRC Press: Boca Raton, FL, 1989; Vol. 1, Chapter 17).

Scheme 2

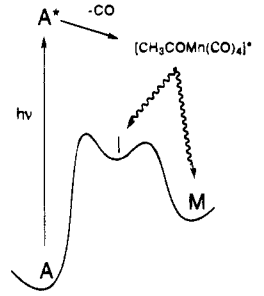

experiment, a plot of k_{obs} vs [L] was linear (slope = (4.0 ± 0.8) × 10^{-5} $M^{-1}s^{-1}$) with an intercept near the origin. Similar behavior was previously observed for the reaction of **M** with *N*-methylcyclohexylamine in *n*-hexane.[4]

Discussion

The 308-nm flash photolysis of **A** leads to photodissociation of CO with moderate efficiency and the "prompt" formation of two primary products within the 100-ns time frame of TRIR observation. The major species initially formed in this manner is the intermediate **I**, which undergoes subsequent methyl migration to **M** in competition with trapping by CO to reform **A** or by another ligand L to give a substituted analog of **A**. The lesser species initially formed is **M**, also seen for photolysis in low-temperature frozen solutions (see above) and matrices.[15] Thus, one may conclude that prompt formation of **M** is one of two reaction channels available for decay of the vibrationally hot species formed by CO dissociation from the initial excited state prepared by 308-nm light (Scheme 2).[25] The same products were found using excitation via photosensitization.

Nature of Intermediate I. The bulk of the present discussion will focus on the reactions and spectra of **I**. When this species is prepared by flash photolysis of **A** in PFMC or cyclohexane, the subsequent reactions with various ligands L (eq 8) , especially CO, are rather sluggish. The low relative reactivity

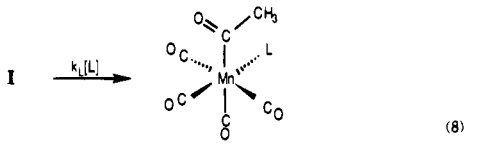

(8)

is emphasized by comparison to the reactivity of the intermediate **X** formed by similar flash photolysis of **M** (eq 9). **X**, which

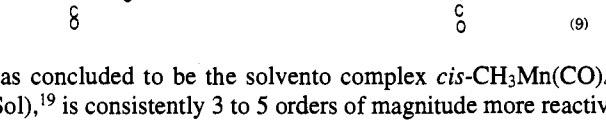

(9)

was concluded to be the solvento complex *cis*-$CH_3Mn(CO)_4$(Sol),[19] is consistently 3 to 5 orders of magnitude more reactive than **I** under analogous conditions except in THF. Furthermore, the k_{CO} values were found to be dramatically more sensitive to the nature of Sol for **X** than for **I** (Table 3). For example, the k_{CO}'s for **X** are 1 × 10^{10} M^{-1} s^{-1} in PFMC, 4.5 × 10^8 M^{-1} s^{-1} in cyclohexane, and 1.4 × 10^2 M^{-1} s^{-1} in THF; the respective values for **I** are 1.5 × 10^4, 6.5 × 10^3, and ~4 × 10^2 M^{-1} s^{-1}. Another worthwhile comparison might be to the reactivity of $Cr(CO)_5$(Sol) generated by flash photolysis of $Cr(CO)_6$ in different solvents. This too shows high sensitivity to the nature of Sol with the respective k_{CO} values being 3 × 10^9, 3.6 × 10^6, and <10 (estimate) M^{-1} s^{-1}.[26]

The logical question is whether the differences between the reactivities of **I** and **X** derive from comparative electronic effects of CH_3 vs CH_3CO, or do they represent a more specialized property of the acyl group? The Hammet σ-constants for these groups[27] clearly show methyl to be considerably more electron donating than acetyl. Despite this, there is no clear pattern of carbonyl ν_{CO} frequencies for the respective intermediates which reflects these different electronic properties. Thus, the ability of the acyl group to chelate the metal with the oxygen of an η^2-bound carbonyl (**C**)[28] or agostic interaction with the methyl group (**B**) is probably the major factor in defining the reactivity differences. Such chelation should be more important in weakly coordinating solvents such as alkanes or perfluoroalkanes than in THF (and certainly DMSO)[3d] in which solvento complexes (**S**) might be expected to dominate (see below). In this context it is notable that NMR experiments with the molybdenum complex $CH_3C(O)Mo(S_2CNMe_2)(CO)(PMe_3)_2$ in CH_2Cl_2 have been interpreted in terms of equilibria between analogs of all three species.[29]

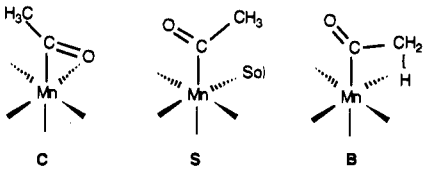

In an earlier communication,[13] we argued that, since ν_{CO} frequencies for **I** were virtually identical in THF and 2,5-Me_2-THF solutions, the acetyl group of this intermediate may have the η^2 configuration even in THF.[13] However, this conclusion was based on the assumption that the latter solvent would be considerably more sterically crowded than THF and would be much less likely to coordinate. Kinetic data now suggest that a species such as **S** may prevail in both solvents (see below). Furthermore, subsequent MM2 calculations here show steric effects to be relatively minor for coordination of *cis*-2,5-Me_2-THF to $CH_3C(O)Mn(CO)_4$ although more significant for *trans*-2,5-Me_2THF. The earlier studies were thus flawed since the 2,5-Me_2THF solvents contained both isomers in ~3/2 *cis/trans* ratio as shown by PMR. Thus, we now conclude that in these two solvents as well as in 2-MeTHF, the predominant species are solvent complexes **S**. Notably, in these solvents, a mixture of *cis*- and *trans*-$CH_3C(O)Mn(CO)_4$(Sol) isomers was observed, possibly formed by trapping the unsaturated species formed by labilization of *cis*- and *trans*-CO in a roughly statistical ratio. The latter isomer rapidly converted to the former. It is not immediately obvious why *trans* **S** isomers were not observed in the hydrocarbon solvents, although the answer may simply be that such species are too reactive to be seen under these conditions.

The same MM2 calculations clearly indicate that Me_4THF is much more sterically crowded in forming a cis complex to

(25) (a) The energy of 308 nm light (~93 kcal mol^{-1}) is twice the dissociation energy of a Mn−CO bond (~44 kcal mol^{-1}). (b) Smith, G. P. *Polyhedron* **1988**, *7*, 1605−1608.

(26) (a) Bonneau, R.; Kelly, J. M. *J. Am. Chem. Soc.* **1980**, *102*, 1220−1221. (b) Kelly, J. M.; Long, C.; Bonneau, R. *J. Phys. Chem.* **1983**, *87*, 3344. (c) The k_{CO} value for $Cr(CO)_5$THF in THF was estimated as being no larger and probably significantly smaller than k_L's (~1 M^{-1} s^{-1}) for reactions with other, more basic ligands (Weiland, S.; van Eldik, R. *Organometallics* **1991**, *10*, 3110−3114).

(27) Hine, J. *Physical Organic Chemistry*, 2nd ed.; McGraw-Hill: New York, 1962; p 87.

(28) Durfee, L. D.; Rothwell, I. P. *Chem. Rev.* **1988**, *88*, 1059−1079.

(29) (a) Carmona, E.; Contreras, L.; Poveda, M. L.; Sanchez, L. J. *J. Am. Chem. Soc.* **1991**, *113*, 4322−4324. (b) Contreras, L.; Monge, A.; Pizzano, A.; Ruiz, C.; Sanchez, L.; Carmona, E. *Organometallics* **1992**, *11*, 3971−3980. (c) Carmona, E.; Sanchez, L.; Marin, J. M.; Poveda, M. L.; Atwood, J. L.; Priester, R. D.; Rogers, R. D. *J. Am. Chem. Soc.* **1984**, *106*, 3214−3222.

$CH_3C(O)Mn(CO)_4$. Interestingly, the ν_{CO} bands of the $\mathbf{I_c}$ intermediate formed in this solvent are significantly higher frequency than the analogous band in THF, indeed are closer to the frequencies seen in cyclohexane. Furthermore, the reactions of $\mathbf{I_c}$ with the ligands $P(OMe)_3$ or 4-Ph-py in Me_4-THF are 2−3 orders of magnitude faster than in THF, and again the observed behavior is more consistent with the analogous intermediate in alkane solution. Certainly one logical explanation is that in this sterically crowded solvent, the predominant form of $\mathbf{I_c}$ is analogous to the species seen in the hydrocarbon and halocarbon solvents, i.e., **C**.

While η^2-acyl chelation (**C**) would appear to be the logical explanation for the relative stability of **I** toward reaction with incoming ligands in weakly coordinating solvents, the agostic chelate **B** cannot be excluded off-hand by the current experiments. However, the former alternative gains support from ab *initio* calculations for the "unsaturated" species $CH_3C(O)Mn(CO)_4$ which demonstrate much greater stability for **C** than for **B** (or for a truly unsaturated species **U**).[30] This conclusion is also consistent with the -59-cm^{-1} shift of the acyl group ν_{CO} band on going from **A** to **I**. While this band (1607 cm^{-1}) is on the high end of the frequency range typically observed for η^2-acyl complexes, the magnitude of the shift is consistent with the differences seen for systems where mono and dihapto acyl arrangements can be compared for similar metal centers.[28] Nonetheless, the acyl ν_{CO} of **I** in THF occurred at a similar frequency. This may be coincidental, given that replacing a *cis*-CO by a stronger σ-donor, weaker π-acceptor such as THF would also be expected to affect that band.

More convincing evidence regarding the nature of **I** in THF comes from examining reaction dynamics differences. Despite the relatively low reactivity of **I** with CO in alkane solution, k_{CO} is significantly smaller in THF. When $P(OMe)_3$ is the incoming ligand, the difference is 3 orders of magnitude between cyclohexane and THF solutions (Table 3). Since the Mn−THF bonds are likely to be >10 kcal/mol stronger than corresponding Mn−alkane interactions,[31] substantial reactivity differences would certainly be expected if **I** were the solvent complex **S** in both media. For example, such effects on the substitution rates were considered diagnostic of solvent coordination in **X**[19] and in $Cr(CO)_5(Sol)$.[26] Alternatively, relatively small differences might be expected if **I** were in the η^2-acyl configuration **C** in both media, although the magnitude of the effects would certainly depend on the role played by solvent in the substitution mechanism (see below). Nonetheless, the fact that **I** is dramatically less reactive toward ligand substitution than is **X** in cyclohexane, but still shows substantial decreases in this reactivity in THF, leads to our conclusion that **I** is the chelate complex **C** in the former medium (and in the other less strongly coordinating solvents in Table 2) and is the solvento species **S** in the latter. Furthermore, the similar reactivities with $P(OMe)_3$ (and with CO) in THF, 2-MeTHF, and 2,5-Me_2THF (Table 4) clearly point to the respective intermediates **I** having similar coordination modes, i.e. as **S**, in these oxygen-donor solvents.

Mechanisms for Reactions of I. Scheme 3 is an attempt to outline possible pathways for the intermediate species formed by flash photolysis of **A**. For convenience, **B** and **U** are represented together since there is no direct evidence for either

Scheme 3. Kinetics Scheme for Reactions of Intermediates

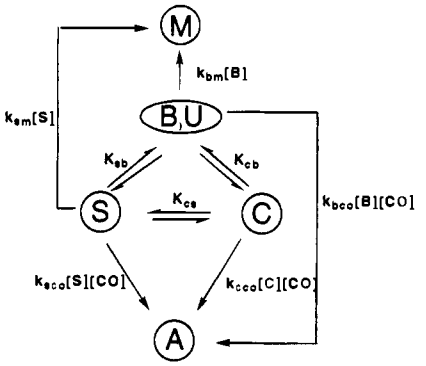

and they are related by a simple rotation of the methyl group into the vacated coordination site. A concerted, direct reaction from **C** to **M** is not shown, since it seems unlikely given the position of the methyl group relative to the coordination site. Two limiting cases will be discussed, example 1 being cyclohexane solution where **C** is the predominant form of **I**, and example 2 being THF solution where **S** predominates. The equilibria and rates of the reactions shown in this scheme can be represented as follows:

$$K_{cb} = \frac{[\mathbf{B}]}{[\mathbf{C}]} \qquad K_{cs} = \frac{[\mathbf{S}]}{[\mathbf{C}]} \qquad K_{sb} = \frac{[\mathbf{B}]}{[\mathbf{S}]} \tag{10}$$

$$-\frac{d[\mathbf{I}]}{dt} = \frac{d[\mathbf{M}]}{dt} + \frac{d[\mathbf{A}]}{dt} = (k_m + k_{co}[CO])[\mathbf{I}] \tag{11}$$

where

$$d[\mathbf{M}]/dt = k_{bm}[\mathbf{B}] + k_{sm}[\mathbf{S}] \tag{12}$$

$$d[\mathbf{A}]/dt = (k_{cco}[\mathbf{C}] + k_{bco}[\mathbf{B}] + k_{sco}[\mathbf{S}])[CO] \tag{13}$$

In cyclohexane (and other weakly coordinating solvents), [**I**] ~ [**C**], so according to this scheme

$$k_{co} = k_{cco} + K_{cb}k_{bco} + K_{cs}k_{sco} \tag{14}$$

$$k_m = K_{cb}k_{bm} + K_{cs}k_{sm} \tag{15}$$

The data of Table 2 demonstrate the k_{CO} path to be relatively insensitive to solvent in the hydrocarbon and halocarbon media, so it is improbable that the $K_{cs}k_{sco}$ term is an important contributor to eq 14. Thus, a likely mechanism would be direct replacement of the η^2-acyl carbonyl by the incoming ligand via an "associative interchange" mechanism or initial rearrangement by "dissociation" of this ligand to give either **B** or **U** followed by rapid reaction with L. The clean second-order behavior of the reaction of **C** with L as well as the marked sensitivity of k_L to the nature of L (e.g. k_L for L = $P(OMe)_3$) = $200k_{CO}$) argues convincingly for the dominant substitution reaction of this species to occur via the interchange mechanism, i.e. $k_{CO} \approx k_{CCO}$.

The microscopic reverse of the direct substitution of a ligand on the η^2-acyl group would be "acyl-assisted" ligand dissociation. Kinetic studies[5b] of the thermal decarbonylation of **A** have shown that the rate determining step is loss of CO from **A**. As the alkyl group on the acyl was varied the rate of the reaction was shown to *increase* with the electron-releasing capability of R, which is consistent with increased capability of the acyl oxygen to donate to the metal center.

In contrast, the methyl migratory pathway of **C** is much more strongly solvent dependent even in these weakly coordinating media. One could argue that this reflects stabilization of a polar

(30) (a) Marynick, D. S. Personal communication to P.C.F. (b) Axe, F. U.; Marynick, D. S. *Organometallics* **1987**, *6*, 572−580. (c) Axe, F. U.; Marynick, D. S. *J. Am. Chem. Soc.* **1988**, *110*, 3728−3734. (d) Ziegler, T.; Versluis, L.; Tschinke, V. *J. Am. Chem. Soc.* **1986**, *108*, 612−617.

(31) Yang G. K.; Vaida, V.; Peters, K. S. *Polyhedron* **1988**, *7*, 1619−1622.

(32) Connor, J. A.; Zafarani-Moattar, M. T.; Bickerton, J.; El Saied, N. I.; Suradi, S.; Carson, R.; Takhin, G. A.; Skiner, H. A. *Organometallics* **1982**, *1*, 1166−1174.

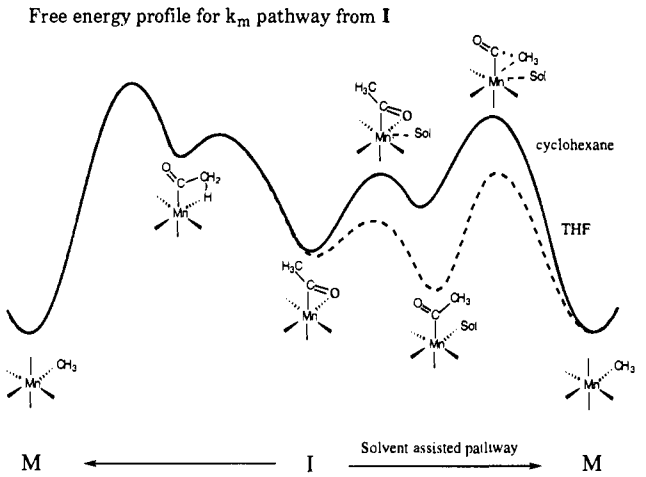

Figure 9. Reaction coordinate diagram for methyl migration via solvent-assisted and unassisted pathways.

transition state, for example in the k_{bm} pathway, by solvents with a higher dielectric constant. But this would not explain the marked difference between the methyl migration rates in cyclohexane and PFMC; thus a more intimate involvement of solvent appears likely. Such a pathway could involve methyl migration occurring from **S** present at low concentrations in equilibrium with **C**, i.e., $k_m \approx K_{cs}k_{sm}$ under these conditions. Since solvent would affect both K_{cs} and k_{sm}, it is not clear that the trend would systematically follow the solvent's coordinating ability, although qualitatively, the trend is essentially consistent (see below).

Figure 9 is an attempt to represent methyl migration in the context of a free energy reaction coordinate diagram. The solid curve describes the case for a weakly coordinating solvent where the η^2-acyl chelate **C** is the most stable form of **I**. Rearrangement of **C** to **B** (perhaps via **U**) is viewed as a less favorable pathway to **M** than is reaction of **C** with solvent to give first the higher energy species **S** followed by methyl migration to give **M**. The solvent-assisted k_m would result from transition state metal−solvent interactions being of greater importance energetically than in **C**. Thus increasing the solvent's coordinating ability lowers ΔG^* and enhances k_m. (This argument assumes there are no major perturbations in outer sphere solvation energies along the reaction coordinate.)

The situation changes when **S** becomes the lowest energy form of **I**, e.g., in THF, [**I**] ~ [**S**], and according to Scheme 3,

$$k_{co} = (K_{cs})^{-1}k_{cco} + K_{sb}k_{bco} + k_{sco} \quad (16)$$

$$k_m = K_{sb}k_{bm} + k_{sm} \quad (17)$$

In this case, the substitution reaction rates of **S** are slow, presumably because of the Mn−THF bond stability, and the reactivity difference between L = $P(OMe)_3$ and CO is only about a factor of 4. Such behavior would imply that Mn−Sol bond breaking is of much greater importance in THF (as certainly would be expected since this sensitivity was an important criterion in assigning the structures of the intermediates in the various media).

Notably, the markedly lower reactivity of **I** in THF (i.e., the THF complex) toward substitution by various ligands is not paralleled by similar decreases in methyl migration rates. Indeed, under otherwise comparable conditions, k_m is essentially identical in THF and cyclohexane (Tables 2 and 4). This too can be discussed in terms of Figure 9. The more strongly solvating THF lowers the transition state energy of the rate-limiting step to form **M**, but since the $\Delta G^{\ddagger}$ for this pathway is the difference in free energy between **S** and the transition state (rather than **C** and the analogous transition state), and the energies of both species are strongly affected by the nature of Sol, **S** likely being the more stabilized. Notably, mono- or dimethyl substitution on THF appears to slow methyl migration. An electronic effect may be responsible; if the methyl is migrating as a carbanion CH_3^- then the more donor solvents should be the less reactive.

Migration Rates etc. for Other Alkyls. The role of the migrating group in determining the migration dynamics was probed by examining the reactivity of the intermediates generated by the flash photolysis of several $RC(O)Mn(CO)_5$ derivatives in cyclohexane. Notably, the intermediates formed for R = CF_3 or CH_2F ($\mathbf{I_{F3}}$ and $\mathbf{I_F}$, respectively) are both considerably more reactive toward trapping by CO and toward alkyl group migration than the intermediate formed by flash photolysis of **A** and concluded to be the η^2-acyl chelated species **C** in alkane solution. The k_{co} and k_m values for the fluorinated species are each several orders of magnitude larger than the respective values for **I**. Since the k_{co} value for $\mathbf{I_{F3}}$ (1.1×10^7 M^{-1} s^{-1}) is comparable to that seen for the reaction of CO with the "unsaturated" intermediate generated by flash photolysis of $CF_3Mn(CO)_5$[19] (presumably *cis*-$CF_3Mn(CO)_4(Sol)$ in analogy to eq 8), a logical conclusion could be that, even in cyclohexane, $\mathbf{I_{F3}}$ and $\mathbf{I_F}$ are solvent complexes analogous to **S**. Thus, the η^2-acyl configuration appears to be destabilized by the electron-withdrawing nature of the fluoroalkyls which should reduce the basicity of the acyl oxygen.

Substitution of CH_3 for CF_3 would also destabilize the agostic interaction in a structure such as **B** given the much greater reluctance for C−F bonds to participate in such bonding to an unsaturated metal center. For this reason, the monofluoroacetyl complex $\mathbf{A_F}$ was examined, since this species has two C−H bonds still available for agostic bonding. That the trifluoro and monofluoro species have very similar reactivities, both substantially different than that of **I**, can be taken as further evidence that **I** has an η^2 structure in alkane solution. Furthermore, the fact that alkyl migration rates in cyclohexane for $\mathbf{I_{F3}}$ and $\mathbf{I_F}$ are similar and are much faster than for **I** argues against agostic interactions stablizing the transition state energy of the k_m step. The very modest changes in k_{co} and k_m values for the intermediates formed from flash photolysis of $CD_3C(O)Mn(CO)_5$ and $C_2H_5C(O)Mn(CO)_5$ also imply minimal importance of a species such as **B** to the energetics of the methyl migration or CO trapping pathways in these cases.

Comparison of Thermal and Photochemical Kinetics Results. As noted above, thermal reaction of $CH_3Mn(CO)_5$ with various nucleophiles displays kinetics behavior consistent with the mechanism depicted in Scheme 1. In a donor solvent such as THF, the pathway involving initial formation of **A′** appears to dominate. Results of the present thermal reaction studies with L = $P(OMe)_3$ are fully in agreement with this model; the k_1 value determined here (8.5×10^{-4} s^{-1} at 25 °C) is equivalent (within experimental uncertainty) to that reported (9.6×10^{-4} s^{-1}) for other L in THF.[4]

In hexane[4] or cyclohexane (this work), the observed kinetics for reaction of **M** with L proved to be strictly second order over the ligand concentrations studied. While this is consistent with a direct nucleophilic attack via the k_3 step in these weaker donor solvents, the alternative pathway would also be kinetically consistent if the constraint $k_{-1} \gg k_2$[L] were met under the experimental conditions. This point will be discussed further.

A crucial (perhaps *the* crucial) question to consider is whether intermediates identified and studied by the above photochemical techniques are indeed relevant to the thermal carbonylation

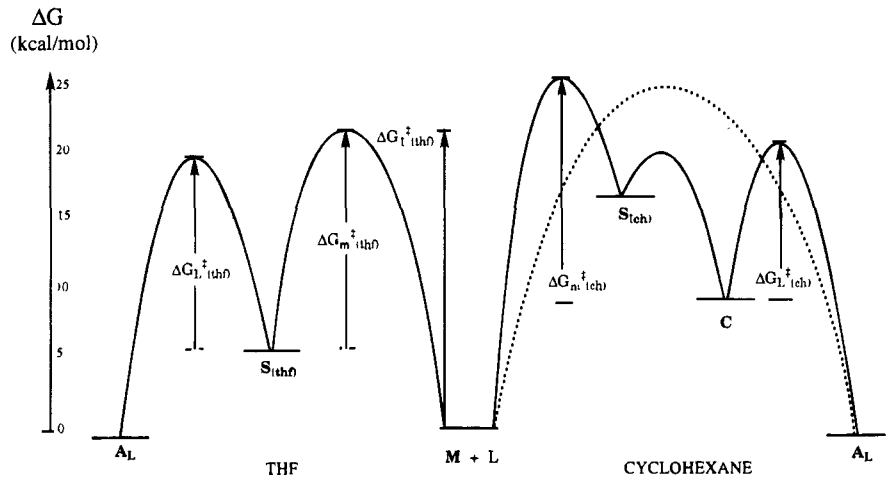

Figure 10. Free energy (ΔG) diagrams for the reaction of $Mn(CO)_5CH_3$ with $P(OMe)_3$ to give *cis*-$CH_3C(O)Mn(CO)_4(P(OMe)_3)$ in cyclohexane (right) and in THF (left). Conditions: 25 °C, $[P(OMe)_3] = 0.1$ M. $\Delta G^{\ddagger}$ values are calculated from the appropriate rate constants at 25 °C. ΔG_{rxn} is approximated as -0.5 kcal mol^{-1} based on an equilibrium constant (23.8 M^{-1}) for reaction of **M** with *N*-methylcyclohexylamine in methanol. Symbols: **M** = $Mn(CO)_5CH_3$, L = $P(OMe)_3$, $\mathbf{S}_{(thf)}$ = $CH_3(O)Mn(CO)_4(THF)$, $\mathbf{S}_{(ch)}$ = $CH_3(O)Mn(CO)_4(c\text{-}C_6H_{12})$, **C** = ($\eta^2$-$CH_3CO)Mn(CO)_4$, $\mathbf{A_L}$ = *cis*-$CH_3C(O)Mn(CO)_4(P(OMe)_3)$, $\Delta G_I^{\ddagger}$(thf) from k_I for thermal carbonylation of **M** in THF with $P(OMe)_3$, $\Delta G_M^{\ddagger}$(thf) from k_m for methyl migration of **I** in THF, $\Delta G_L^{\ddagger}$(thf) from k_{obs} for trapping of **I** with 0.1 M $P(OMe)_3$ in THF, $\Delta G_M^{\ddagger}$(ch) from k_m for methyl migration of **I** in cyclohexane, $\Delta G_L^{\ddagger}$(ch) from k_{obs} for trapping of **I** with 0.1 M $P(OMe)_3$ in cyclohexane. The dashed curve on the right side represents the direct reaction of $P(OMe)_3$ with **M** to give $\mathbf{A_L}$ in cyclohexane. (Please note that k_{obs} ($\Delta G^{\ddagger}$) values for second-order processes will be dependent on [L].)

kinetics. If so, then species **I** generated by flash photolysis of **A** in THF should be the same as species **A′** shown (by kinetics behavior) to be involved in the thermal carbonylation of **M** in THF. If the two intermediates are the same, they should have identical reactivities with various substrates regardless of the manner by which they were generated. Thermal kinetics can determine only rate constant ratios for processes by which a steady state intermediate partitions between different reaction trajectories; e.g., k_{-1}/k_2 is calculated from the slope/intercept ratio of the linear double reciprocal (k_{obs}^{-1} vs $[L]^{-1}$) plot. Our data for reaction of **M** with $P(OMe)_3$ in THF give $k_{-1}/k_2 = (6.6 \pm 1.3) \times 10^{-3}$ M. By contrast, the photochemical experiment allows one to determine the individual reaction rate constants k_m and k_L for the intermediate **I** independently. If **I** and **A′** are the same, then k_m is k_{-1} and k_L is k_2; therefore, k_m/k_L and k_{-1}/k_2 should be equal. The photochemical experiment gives a k_m/k_L value ($5.5 \pm 1.5 \times 10^{-3}$ M), within experimental uncertainty the same as determined for k_{-1}/k_2. Thus, the assertion that the intermediates generated in this manner are relevant to thermally induced migratory insertion is strongly supported.

The photochemically derived rate constants for **I** in cyclohexane clarify the ambiguity noted above in considering the reaction of **M** with strong nucleophiles in alkane solution. The values of k_m and k_L measured for **I** in cyclohexane demonstrate that the condition $k_m \gg k_L[L]$ is not met for the reaction of **M** with excess $P(OMe)_3$ in cyclohexane ($k_m = 9.0$ s^{-1}, $k_L = 1.4 \times 10^6$ M^{-1} s^{-1}, $[L] = 0.006-0.15$ M). Thus, the most plausible explanation of the second-order kinetics in alkanes is that the reaction proceeds via the k_3 step, presumably involving associative attack of L on the Mn, although a less direct pathway such as nucleophilic activation of a carbonyl is difficult to exclude.[5c,33]

The sensitivity of k_1 to the donor properties of the solvent has been rationalized in terms of solvent-assisted methyl migration.[4] If so, both the k_1 and k_3 steps can be viewed as nucleophile-assisted migratory insertion to give a metal acyl intermediate **A′** or product $\mathbf{A_L}$, The slope of the linear k_{obs} (for $\mathbf{A_L}$ formation) vs $[P(OMe)_3]$ plot is k_3 and equals $(4.0 \pm 0.8) \times 10^{-5}$ M^{-1} s^{-1} in cyclohexane, comparable to the k_3 (2.7×10^{-5} M^{-1} s^{-1}) determined for cyclohexylamine in hexanes.[4] For comparison, one can estimate a second-order rate constant for reaction of **M** with THF in that solvent via dividing k_1 by [THF] (12.3 M). Doing so gives $k_{thf} = 6.9 \times 10^{-5}$ M^{-1} s^{-1}. A similar comparison has been drawn by Bergman in discussing carbonylation of (η^5-$C_5H_5)Mo(CO)_3Me$.[5a]

The thermal and photochemical kinetics data can be combined to generate the free energy surfaces depicted in Figure 10 for migratory CO insertion into a $Mn-CH_3$ bond in the presence of 0.1 M $P(OMe)_3$ in THF or cyclohexane. For each, the free energy of **M** was arbitrarily set at zero as the reference point, and solvent-dependent solvation energy differences between **M** and **A** were ignored. The reaction was proposed to proceed from **M** to **S** to **C** to the substituted acyl complex $\mathbf{A_L}$ in cyclohexane and from **M** to **S** to $\mathbf{A_L}$ in THF. The ΔG_{rxn} for overall reaction to form $\mathbf{A_L}$ was estimated to be -0.5 kcal mol^{-1} based on the known equilibrium constants for L = *N*-methylcyclohexylamine;[4] however, the exact position is not critical to discussion of the intermediates. For reaction in THF, the first barrier was calculated from k_1(thf) (8.5×10^{-4} s^{-1}, $\Delta G_I^{\ddagger}$(thf) = 21.6 kcal mol^{-1}) determined in the thermal carbonylation experiment. The principle of microscopic reversibility requires that, if **I** (i.e., **S**(thf)) observed photochemically and **A′** from the thermal experiment are the same, the k_1 and k_{nt} steps have the same transition state. Thus, the position of **S**(thf) was calculated from $\Delta G_I^{\ddagger}$(thf) $-$ $\Delta G_m^{\ddagger}$(thf) = 5.5 kcal mol^{-1} above **M**. The barrier for reaction of **S**(thf) with L was derived from the pseudo-first-order rate constant in the presence of 0.1 M $P(OMe)_3$ ($k_{obs} = k_L[L] = 1.7 \times 10^2$ s^{-1}, $\Delta G_L^{\ddagger}$(thf) = 14.4 kcal mol^{-1}).

For the corresponding cyclohexane diagram, the $\Delta G_I^{\ddagger}$(ch) barrier for reaction of **M** with solvent could not be directly extracted from the experimental data. Instead, the *lower limit* for the barrier height was approximated from an estimate of the free energy difference ΔG_C(ch) between **C** and **M** plus the $\Delta G_m^{\ddagger}$(ch) measured by flash photolysis. The equilibrium constant between **M** and **C** in aromatic hydrocarbons was estimated by dividing the k_1 (2.2×10^{-6} s^{-1}) determined in mesitylene by Mawby et al.[4] by the k_m (6.7 s^{-1}) reported here for benzene solution (Table 2), $K_{est} = k_1/k_m = 3.3 \times 10^{-7}$. Since solvation energy differences between **M** and **C** should be similar

(33) Ford, P. C.; Rokicki, A. *Adv. Organomet. Chem.* **1988**, *28*, 139–217.

for aromatic and aliphatic hydrocarbons solutions, this K provides the estimated free energy difference between **C**(ch) and **M**(ch), $\Delta G_C(ch) = +8.9$ kcal mol^{-1}. In cyclohexane k_m-(ch) = 9.0 s^{-1} ($\Delta G_m^{\ddagger}(ch) = 16.1$ kcal mol^{-1}); accordingly, the barrier for the reverse reaction would be $\Delta G_1^{\ddagger}(ch) = \Delta G_C(ch) + \Delta G_m^{\ddagger}(ch) = 25.0$ kcal mol^{-1}. This corresponds to a hypothetical $k_1(ch)$ value in cyclohexane of 1.2×10^{-6} s^{-1}, about half that determined for mesitylene.[4] The barrier for reaction of **C**(ch) with L was derived from the calculated first-order rate constant in the presence of 0.1 M $P(OMe)_3$ ($k_{obs} = k_L[L] = 1.4 \times 10^5$ s^{-1}; $\Delta G_L^{\ddagger}(ch) = 10.4$ kcal mol^{-1}).

The free energy of the hypothetical solvento species **S**(ch) (not observed in cyclohexane) should be above that of **S**(thf) by the difference in Mn−solvent bond strengths (assuming entropic differences are small). This difference can be estimated as ~12 kcal mol^{-1},[31] which would place **S**(ch) about 7.6 kcal mol^{-1} above **C**(ch). Barriers for interconversion between the solvento and η^2-acyl intermediates are unknown, but should be low, especially for Sol = cyclohexane.

The above estimate of $\Delta G_1^{\ddagger}(ch)$ is about 4 kcal mol^{-1} higher than $\Delta G_1^{\ddagger}(thf)$, thus the effect of solvent on the barrier for methyl migration (**M** → **I**) is substantial but is significantly attenuated from energy differences estimated for the full Mn−Sol bonds. In contrast, the reverse reactions (k_m steps) show little difference between cyclohexane and THF rates owing to **C** being the dominant form of the intermediate in the former case, **S** in the latter.

The barrier for the direct reaction between **M** and 0.1 M $P(OMe)_3$ in cyclohexane was derived from the experimentally determined second-order rate constant ($k_{obs} = k_3[L] = 4.0 \times 10^{-6}$ s^{-1}; $\Delta G_3^{\ddagger}(ch) = 24.5$ kcal mol^{-1}). The prediction that the lower limit for the $k_1(ch)$ barrier should occur 0.5 kcal mol^{-1} *higher* than that of the direct pathway agrees with the observation that the k_3 pathway operates under this specific set of conditions. Of course, the barrier to the direct pathway will depend critically on the nucleophilicity of L, and in most catalytic processes, L typically is CO. The greatly diminished nucleophilicity of CO relative to $P(OMe)_3$ suggests that when L = CO the solvent-assisted pathway should be significant even in alkane solutions.

Summary

The TRIR and TRO and thermal reaction kinetics studies described here have led to the following observations and conclusions regarding the mechanism for carbonylation of the metal−alkyl bond in $CH_3Mn(CO)_5$ and related species.

(1) The spectroscopic and kinetic results obtained from TRIR and TRO experiments establishe the role of solvent in determining the structure of the "unsaturated" intermediate **I** formed by CO photodissociation from **A**: η^2-acyl chelation was found in weakly coordinating solvents, but solvent coordination predominated in stronger donors. Fluorine substitution on the acyl group apparently destabilized the η^2-chelate form of the intermediate.

(2) Quantitative comparisons of reactivity patterns of photochemically generated intermediates with those predicted from thermal kinetic data substantiate the view that these intermediates are indeed relevant to the thermal reaction mechanisms.

(3) The methyl migration kinetics delineated for the various intermediates indicate the role of solvent assistance in the migration mechanism, even for those media where the lower energy form of **I** is the η^2-acyl chelate complex. These data validate arguments based on thermal reaction data that such solvent assistance plays a key role in the microscopic reverse, the carbonylation of $CH_3Mn(CO)_5$.

Acknowledgment. This research was sponsored by a grant (DE-FG03-85ER13317) to P.C.F. from the Division of Chemical Sciences, Office of Basic Energy Sciences, U.S. Department of Energy. Some laser flash photolysis experiments were carried out on a time resolved optical system constructed with support from a U.S. Department of Energy University Research Instrumentation Grant (No. DE-FG05-91ER79039). The able assistance of Brian Lee of this Department in the care of the TRIR apparatus contributed significantly to the success of these studies. Preliminary experiments on this system were initiated by David Ryba and Simon Belt.

JA950204T